materials proceedings

Proceeding Paper

The Effect of Preconditioning Temperature on Gas Permeability of Alkali-Activated Concretes †

Patrycja Duży [1,2,*], Marta Choinska Colombel [2], Izabela Hager [1] and Ouali Amiri [2]

1 Chair of Building Materials Engineering, Faculty of Civil Engineering, Cracow University of Technology, 31-155 Cracow, Poland
2 Research Institute in Civil and Mechanical Engineering GeM—UMR CNRS 6183, IUT Saint-Nazaire, Nantes University, 44600 Saint-Nazaire, France
* Correspondence: patrycja.duzy@doktorant.pk.edu.pl
† Presented at the 10th MATBUD'2023 Scientific-Technical Conference "Building Materials Engineering and Innovative Sustainable Materials", Cracow, Poland, 19–21 April 2023.

Abstract: Alkali-activated materials (AAMs) are a group of environmentally friendly binders considered alternatives to conventional cementitious binders. They utilise industrial wastes such as slag and fly ash to reduce cement production and related CO_2 emissions. Despite the strong interest of researchers, the application of alkali-activated concrete (AAC) in constructions is still very limited. Given the difference in the process of producing the AAC and ordinary Portland cement concrete (OPCC), some of the testing methods need to be adjusted to a new type of binder. The increased sensitivity of AAM to high temperatures leads to discussions on the results achieved in the gas permeability tests that require the samples to be dried first. In this paper, the influence of drying temperature applied to the samples on the gas permeability will be presented. The binders' precursors are blends of fly ash (FA) and ground granulated blast furnace slag (GGBFS) in slag proportions of 5%, 20%, and 35%, expressed by the mass of FA. Materials are denoted AAC5, AAC20, and AAC35, respectively. Measurements of the gas permeability of concretes were conducted by the RILEM–CEMBUREAU method, with lab adaptation for gas flow measurements. The comparison of results obtained shows the increase in gas permeability values with the temperature. However, the corresponding effect of temperature on permeability is driven by, on the one hand, the binder composition, and on the other hand, the aggregate's nature.

Keywords: gas permeability; geopolymer concrete; temperature impact; drying

Citation: Duży, P.; Choinska Colombel, M.; Hager, I.; Amiri, O. The Effect of Preconditioning Temperature on Gas Permeability of Alkali-Activated Concretes. *Mater. Proc.* **2023**, *13*, 38. https://doi.org/10.3390/materproc2023013038

Academic Editors: Katarzyna Mróz, Tomasz Tracz and Tomasz Zdeb

Published: 20 February 2023

1. Introduction

Concrete, as one of the most commonly used construction materials, is exposed to plenty of aggressive environmental factors [1]. Transport of external media is conducted by a connected pore structure [2]. This is the reason why the description of the pore network deserves special attention in the analysis of concrete's durability [3,4].

Gas permeability is one of the parameters that describes the pore structure of materials, therefore, it is considered one of the most popular parameters to determine their quality and durability [3,5]. Among the variety of methods used to determine the gas permeability, the most common are the CEMBUREAU method [6] and the oxygen permeability index. The principle of these tests is to measure the amount of gas passing through the sample with a known cross-sectional area per unit of time. The most commonly used gases are oxygen, nitrogen, or dry air. These methods of measurement refer to laboratory tests. In situ testing by Figg's method [7] or others methods described in the literature [8,9] is acceptable but the main disadvantage of them is the lack of possibility to control the impact of temperature and of moisture on the material. These parameters strongly affect the result of permeability measurements [10,11].

Gas permeability measurements are basic to the determination of the durability of constructions and modelling the service life [12]. The CEMBUREAU method is considered a reference method for air permeability for other methods. However, laboratory methods require temperature preconditioning of the specimens [6,13]. The temperature of drying ranges from 50 °C to 105 °C. It is clear that the results of measurements will not be the same for variable conditions. The definition of the temperature impact on the results obtained may allow researchers to adjust the condition to the tested materials and compare it with others.

The temperature impact on geopolymers' microstructure is the subject of many investigations [14,15]. Many of them focus on behaviour in high temperatures up to 1000 °C. [16,17]. However, it is a well-known fact that the temperature of curing strongly affects geopolymer properties, especially alkali-activated fly ashes [18,19]. In addition, for alkali-activated slag, temperature of curing influences its microstructure and porosity [20]. Taking into consideration the influence of preconditioning of specimens on gas permeability, the question about its applicability to geopolymer concretes is an unsolved problem.

The temperature that activates fly ashes has been investigated by many researchers in recent years [21,22]. Palomo et al. [23] presented the evolution of properties of alkali-activated fly ash cured at temperatures between 65 °C and 85 °C. The ingress of compressive strength with high temperature reached 60 MPa. With these changes, it is obvious to assume that all the properties connected with porosity were also affected by curing temperature. These studies only confirmed the theories made much earlier [24]. Similar research was conducted to define the influence of the activator used [25] for mixes and their behaviours in temperatures between 75 °C and 95 °C. Unfortunately, there is no possibility to specify one general rule to describe the influence of curing temperature on porosity and microstructure of alkali-activated materials. It depends on the type of precursor and activator and on the temperature applied. In the case of gas permeability measurement, it is more necessary to compare the results obtained for materials with different compositions than to obtain accurate values of permeability. In this paper, the influence of preconditioning temperature on gas permeability measurements and comparison of this influence on different compositions of alkali-activated concretes are presented.

2. Materials

The studies were conducted on six compositions of alkali-activated concretes based on fly ash (Połaniec powerplant, Poland) with ground granulated blast furnace slag (Ekocem Dąbrowa Górnicza, Poland) replacement by mass. Three levels of GGBFS dosage were examined: 5%, 20%, and 35%. Two types of coarse aggregate were used to detect its influence on gas permeability. The tested blends were denoted AAC5B, AAC20B, and AAC35B for basalt aggregate and AAC5D, AAC20D, and AAC35D for dolomite aggregate with 5%, 20%, and 35% of slag, respectively. According to ASTM C618 Standard Specification for Coal Fly Ash and Raw or Calcined Natural Pozzolan for Use in Concrete [26], the FA was categorised as class F, and is mainly composed of silicon dioxide and aluminium oxide. In the case of the slag used, it mainly consists of calcium oxide and silicon oxide. The chemical compositions of precursors are presented in Table 1. For activation, the diluted sodium silicate solution Geosil® 34417, supplied by Woellner, was used.

Table 1. Oxide composition of fly ash and ground granulated blast furnace slag.

wt.%	SiO_2	Al_2O_3	Fe_xO_y	CaO	MgO	SO_3	K_2O	Na_2O	P_2O_5	TiO_2	Mn_3O_4	Cl^-
FA	52.30	28.05	6.32	3.05	1.71	0.28	2.51	0.76	0.69	1.35	0.07	-
GGBFS	39.31	7.61	1.49	43.90	4.15	0.51	0.36	0.47	-	-	-	0.04

The mixing procedure was performed based on prior experience of the research group [27]. The first step was to prepare pastes. Fly ash was mixed with diluted alkaline solution until a homogenous consistency was obtained. Slag was added with constant stirring. At that time, a mixture of coarse aggregate (basalt or dolomite) and quartz sand was prepared in a larger mixer. When the paste was ready, it was added to the mixer with the aggregate and distributed evenly throughout the mass. The samples were cast and compacted on a shaking table in cylindrical moulds with diameter 11 cm and height 22 cm. They were stored in ambient conditions at 20 ± 2 °C and protected from water evaporation by plastic film. For the prepared samples, no thermal curing was applied.

3. Methods

The CEMBUREAU method is still one of the most popular methods of gas permeability measurements [28]. The values of inlet and outlet pressures are steady during the measurement. Identification of gas permeability is based on stabilised permanent gas flow. The atmospheric pressure and temperature, which may affect the results, are also taken into account for permeability estimation. Lateral pressure of 8 bars is applied to the rubber gum surrounding the specimen to exclude gas leaking around the sample.

Measurements in accordance with this standard were initially carried out within samples which had never been dried before. The value of gas permeability started to stabilise after 240 days and this continued for up to 360 days, as given in Figure 1.

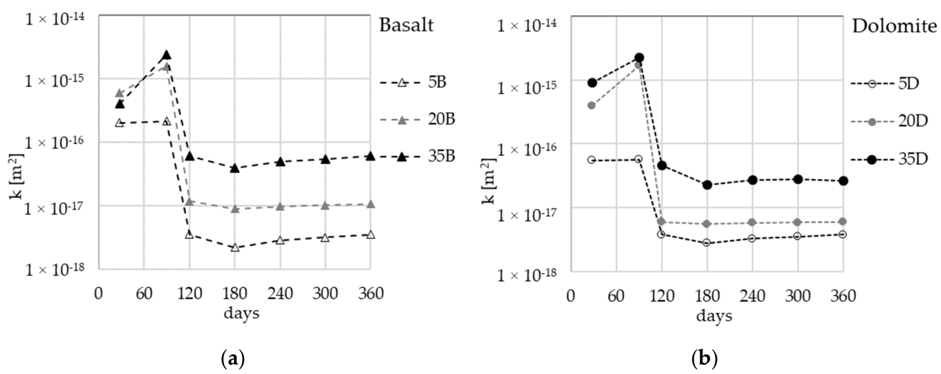

Figure 1. Gas permeability development in time for samples stored in room conditions: (**a**) basalt aggregate; (**b**) dolomite aggregate.

In order to exclude test disturbance caused by the age of the materials, the impact of preconditioning temperature started to be investigated once the values of permeability stabilised (after 1 year). AAMs are highly sensitive to external temperature application. Referring to this fact, three temperatures of preconditioning were taken into consideration: 40 °C, 80 °C, and 105 °C.

After the first step, corresponding to the measurement performed on the natural state of the material (denoted as 20 °C, corresponding to data at 360 days, see Figure 2), further stages of research were run. For each step of temperature, the drying process was carried out in order to reach a stable mass of samples (relative mass loss Δm less than 0.1% during 24 h). In order to cool down the specimens, they were placed in a desiccator fulfilled with hydrophobic pellets to reduce moisture. After 24 h of cooling down, the mass of each material was verified. Then, the permeability test was performed. For each material, two specimens were tested. Just after measurements, the specimens were placed in a dryer at the next level of temperature and the procedure was repeated. All of the tests were conducted on the same specimens to avoid impact of heterogeneity of concretes. The total drying process and changes in specimens' mass are shown in Figure 2.

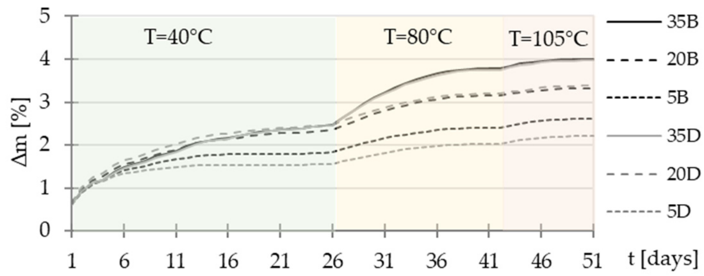

Figure 2. Scheme of drying process.

The values of gas permeability coefficients were calculated according to modified Darcy's law. The analysis of the obtained results consists of influence of temperature on the values of apparent and intrinsic gas permeability and the occurrence of boundary slippage effect related to the Klinkenberg effect [29].

4. Results and Discussion

Apparent permeabilities as a function of inversed mean pressure show permeability increased with temperature and followed Klinkenberg's law. The pore fineness increased, probably because of the creation of newly accessible fine pores during drying and cooling. In parallel, a competitive action is normally due to expansion of already present and accessible pores, caused by water evaporation from internal surfaces [30,31].

Table 2 presents intrinsic permeability values for initial, not oven-dried, specimens (20°C) of all the tested concretes. These intrinsic permeabilities were calculated following Klinkenberg's law, using apparent permeabilities. The values for low slag content materials (AAC5) are the lowest, independently of aggregate type, in comparison to other materials. Globally, there is no tendency in permeability evolution as a function of aggregate type.

Table 2. The intrinsic permeability values for specimens preconditioned at 20 °C.

	AAC5B	AAC20B	AAC35B	AAC5D	AAC20D	AAC35D
k_{20} [m^2]	3.53×10^{-18}	1.08×10^{-17}	6.07×10^{-17}	3.81×10^{-18}	6.00×10^{-18}	4.65×10^{-17}

The analysis presented below is based on intrinsic gas permeability values and the relation between them for appropriate drying temperatures. The ratio proposed for the further analysis is k_i/k_y, where i, y mean drying temperatures. Values of k_i/k_{20} are shown in Figure 3.

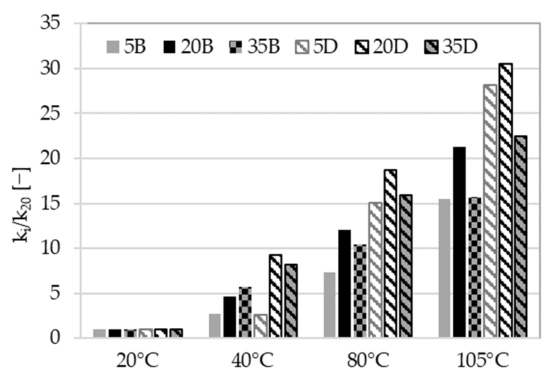

Figure 3. Values of k_i/k_{20} ratios for temperatures of preconditioning.

For almost all of the temperatures (40, 80, 105 °C), the values of permeability for dolomite-based concrete increased more than for basalt-based concrete. This behaviour is probably due to physical changes in the microstructure of the zone between paste and aggregate, as the latter is not intrinsically impacted at these temperatures. The impact of the drying process at 40 °C is much higher for AAC35B and AAC35D than for AAC5B and AAC5D, which is clearly visible in Figure 4. For AAC35B, the value of permeability increased from 6.07×10^{-17} m^2 to 34.8×10^{-17} m^2 for 20 °C and 40 °C, respectively (the k_{40}/k_{20} ratio was equal to 5.74). For AAC35D, permeability at these temperatures reached 4.65×10^{-17} m^2 and 38.2×10^{-17} m^2, making the k_{40}/k_{20} ratio equal to 8.22. However, low slag content materials show lower sensitivity when heated to a temperature of 40 °C. The values of the k_{40}/k_{20} ratio for AAC5B and AAC5D were 2.71 and 2.64, respectively. The impact of the drying process at over 40 °C is related to complex physical and chemical changes and will be discussed below.

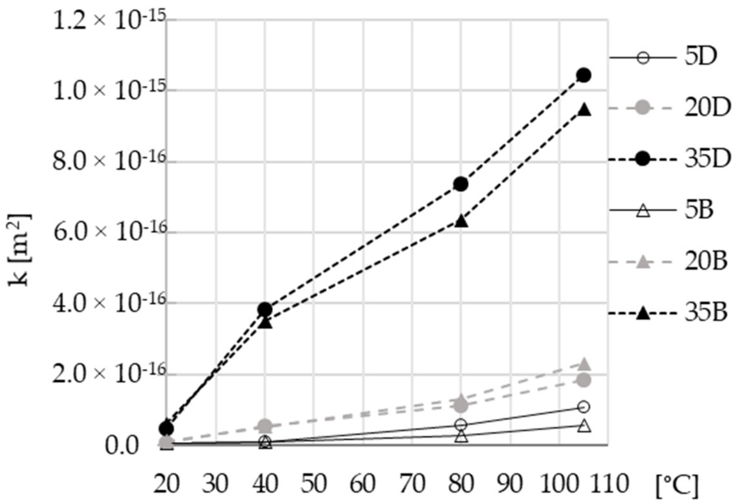

Figure 4. Impact of drying temperature on gas permeability of AAC.

Materials with the highest amount of fly ashes reveal a significant response to temperatures between 40 °C and 105 °C. As was explained in the Introduction, these materials are sensitive to temperature treatment. On the one hand, this may be due to the activation of the FA and therefore the creation of new phases, but on the other hand, it may be due to a rapid release of water from the pores of the material and generation of microcracks in the material, amplifying gas flow. All the absolute values of gas permeability are summed up in Figure 4.

As the results presented before are mainly related to aggregates' nature, the results presented in Figure 4 are strongly focused on slag content impact. Three families of results, depending on slag amount, may be highlighted. In the case of 5% and 20% slag content, the influence of the drying temperature is slight in comparison to 35% slag. Thermal expansion strain differences between high-content slag paste and aggregate should be more significant than for other pastes. It provides geometrical incompatibilities and therefore probably microcracking, causing an increase in permeability of up to two orders of magnitude.

The analysis carried out has brought many valuable observations. The difference in drying temperature impact shows distinct sensitivity of materials to drying. Furthermore, a meaningful impact of slag addition is highlighted.

5. Conclusions

The tests carried out were aimed at comparing the influence of the sample preconditioning temperature on the result of the gas permeability test. The variety of standards used for measurements may significantly affect the obtained result, which has been proven in this paper. Based on the obtained experimental results, the following conclusions can be drawn:

- The drying temperature of the samples significantly affects the obtained permeability values.

- The effect of temperature on AAC permeability is strongly related to the precursor used and especially to the slag content.
- All permeability test reports have to include sample preconditioning conditions to enable correct interpretation of results.
- The gas permeability value of materials with the same binder can be compared under the same conditions, taking into account the impact of the aggregate and the quality of the zone between aggregate and paste.
- The results of permeability tests carried out on AAC samples with different binders under different sample moisture conditions should not be compared.

Experimental research has clarified the possibility of comparing the results obtained for materials with different binders and aggregates. Conclusions drawn from these studies may provide guidance for further analysis and interpretation of permeability test results performed on alkali-activated concrete.

Author Contributions: Conceptualisation, I.H., M.C.C. and O.A.; methodology, M.C.C. and P.D.; validation, I.H. and O.A.; formal analysis, M.C.C. and I.H.; investigation, P.D.; data curation, P.D. and M.C.C.; writing—original draft preparation, P.D. and M.C.C.; writing—review and editing, M.C.C., I.H., O.A. and P.D.; visualisation, P.D. and M.C.C.; supervision, M.C.C.; project administration, I.H.; funding acquisition, I.H. and M.C.C. All authors have read and agreed to the published version of the manuscript.

Funding: The authors of this research were financially supported by SMART-G Smart Geopolymers project financed by National Centre for Research and Development (NCBR)–ERA-MIN2-3/SMART-G/1/2022.

Data Availability Statement: The data presented in this study are available on request from the corresponding author.

Acknowledgments: The publication cost of this paper was covered with funds of the Polish National Agency for Academic Exchange (NAWA): "MATBUD'2023–Developing international scientific cooperation in the field of building materials engineering" BPI/WTP/2021/1/00002, MATBUD'2023.

Conflicts of Interest: The authors declare no conflict of interest.

References

1. Bernal, S.A.; Bílek, V.; Criado, M.; Fernández-Jiménez, A.; Kavalerova, E.; Krivenko, P.V.; Winnefeld, F. Durability and testing—Degradation via mass transport. In *RILEM State-of-the-Art Reports: Alkali Activated Materials*; Provis, J.L., van Deventer, J.S.J., Eds.; Springer: Dordrecht, The Netherlands; Heidelberg, Germany; New York, NY, USA; London, UK, 2014; Volume 13, pp. 223–276.
2. Li, K.F. *Durability Design of Concrete Structure: Phenomena, Modeling and Application*; Wily & Sons: London, UK, 2016.
3. Beushausen, H.; Luco, L.F. *Performance-Based Specifications and Control of Concrete Durability, RILEM State-of-the-Art Reports RILEM TC 230-PSC*; Springer: Dordrecht, The Netherlands, 2016.
4. Stanish, K.D.; Hooton, R.D.; Thomas, M.D. *Testing the Chloride Penetration Resistance of Concrete: A Literature Review*; FHWA Contract DTFH61-97-R-00022; Department of Civil Engineering University of Toronto: Toronto, ON, Canada, 2001.
5. AKatz, J.; Thompson, A. Quantitative prediction of permeability. *Phys. Rev.* **1986**, *34*, 8179–8181.
6. Kropp, J. Permeability of Concrete as a Criterion of its Durability. *Mater. Struct.* **1999**, *32*, 5.
7. Cather, R.; Figg, J.W.; Marsden, A.F.; O'Brien, T.P. Improvements to the figg method for determining the air permeability of concrete. *Mag. Concr. Res.* **2015**, *36*, 241–245. [CrossRef]
8. Kropp, J.; Hilsdorf, H.K. *Performance Criteria for Concrete Durability, State-of-the-Art Report of RILEM TC116-PCD*; E&FN Spon: London, UK, 1995.
9. Yang, K.; Basheer PA, M.; Bai, Y.; Magee, B.J.; Long, A.E. Development of a new in situ test method to measure the air permeability of high performance concretes. *NDT Int.* **2014**, *64*, 30–40. [CrossRef]
10. Romer, M. Effect of moisture and concrete composition on the Torrent permeability measurement. *Mater. Struct.* **2005**, *38*, 541–547. [CrossRef]
11. Zhang, D.; Li, K. Concrete gas permeability from different methods: Correlation analysis. *Cem. Concr. Compos.* **2019**, *104*, 103379. [CrossRef]
12. Alexander, M.G. Service life design and modelling of concrete structures–background, developments, and implementation. *Revista Alconpat* **2018**, *8*, 224–245. [CrossRef]
13. *XP P18-463*; French Standards, Concretes–Gas Permeability Test on Hardened Concrete. AFNOR: St. Denis, France, 2011.

14. Sitarz, M.; Hager, I.; Kochanek, J. Effect of High Temperature on Mechanical Properties of Geopolymer Mortar. *MATEC Web Conf.* **2018**, *163*, 06004. [CrossRef]
15. Criado, M.; Palomo, A.; Fernández-Jiménez, A. Alkali activation of fly ashes. Part 1: Effect of curing conditions on the carbonation of the reaction products. *Fuel* **2005**, *84*, 2048–2054. [CrossRef]
16. Dudek, M.; Sitarz, M. Analysis of changes in the microstructure of geopolymer mortar after exposure to high temperatures. *Materials* **2020**, *13*, 4263. [CrossRef]
17. Poornima, N.; Revathi, T.; Sivasakthi, M.; Jeyalakshmi, R. Effect of curing on mechanical strength and microstructure of fly ash blend GGBS geopolymer, Portland cement mortar and its behavior at elevated temperature. *Mater. Today Proc.* **2021**, *47*, 863–870. [CrossRef]
18. Runci, A.; Serdar, M. Effect of curing time on the chloride diffusion of alkali-activated slag. *Case Stud. Constr. Mater.* **2022**, *16*, e00927. [CrossRef]
19. Noushini, A.; Castel, A. The effect of heat-curing on transport properties of low-calcium fly ash-based geopolymer concrete. *Constr. Build. Mater.* **2016**, *112*, 464–477. [CrossRef]
20. Chi, M. Effects of dosage of alkali-activated solution and curing conditions on the properties and durability of alkali-activated slag concrete. *Constr. Build. Mater.* **2012**, *35*, 240–245. [CrossRef]
21. Swanepoel, J.C.; Strydom, C.A. Utilisation of fly ash in a geopolymeric material. *Appl. Geochem.* **2022**, *17*, 1143–1148. [CrossRef]
22. Fernandez-Timenez, A.; Palomo, A. Alkali-activated fly ashes: Properties and characteristics. In Proceedings of the 11th ICCC 3, Durban, South Africa, 11–16 May 2003; pp. 1332–1340.
23. Palomo, A.; Grutzeck, M.W.; Blanco, M.T. Alkali-activated fly ashes, a cement for the future. *Cem. Concr. Res.* **1999**, *29*, 1323–1329. [CrossRef]
24. Jiang, W.; Roy, D. Hydrothermal processing of new fly ash cement. *Ceram. Bull.* **1990**, *71*, 642–647.
25. Bakharev, T. Geopolymeric materials prepared using Class F fly ash and elevated temperature curing. *Cem. Concr. Res.* **2005**, *35*, 1224–1232. [CrossRef]
26. *ASTM C618-19*; Standard Specification for Coal Fly Ash and Raw or Calcined Natural Pozzolan for Use in Concrete. ASTM International: West Conshohocken, PA, USA, 2019.
27. Hager, I.; Sitarz, M.; Mróz, K. Fly-ash based geopolymer mortar for high-temperature application–Effect of slag addition. *J. Clean. Prod.* **2021**, *316*, 128168. [CrossRef]
28. Kollek, J.J. The determination of the permeability of concrete to oxygen by the Cembureau method—A recommendation. *Mater. Struct.* **1989**, *22*, 225–230. [CrossRef]
29. Lide, D.R.; Frederikse, H.P.R. *CRC Handbook of Chemistry and Physics*, 84th ed.; CRC Press LLC: New York, NY, USA, 2003; p. 1004.
30. Zhang, J.; Jin, T.; He, Y.; Wang, Y.; Gao, Y.; Zhang, Y. The slippage effect of concrete gas permeability and the influence of its microstructure. *Constr. Build. Mater.* **2022**, *333*, 127384. [CrossRef]
31. Choinska, M. *Effets de la Température, du Chargement Mécanique et de Leurs Interactions sur la Perméabilité du Béton de Structure*; Matériaux. Ecole Centrale de Nantes (ECN); Université de Nantes: Nantes, France, 2006; p. 185.